



STROBOSCOPIC DIFFRACTION IMAGING OF HIGH-FREQUENCY SURFACE ACOUSTIC WAVES

E. ZOLOTUYABKO¹, D. SHILO¹, W. SAUER², E. PERNOT^{3,4} AND J. BARUCHEL³

¹ TECHNION, ISRAEL INSTITUTE OF TECHNOLOGY, HAIFA (ISRAEL)

² LMU MÜNCHEN, (GERMANY)

³ ESRF, EXPERIMENTS DIVISION

⁴ INPG, GRENOBLE (FRANCE)

Surface acoustic waves (SAWs) are widely used in communication systems. The visualization of the wavefronts is important because it gives clues about the defect-related dissipation of acoustic energy, which is detrimental for the device efficiency.

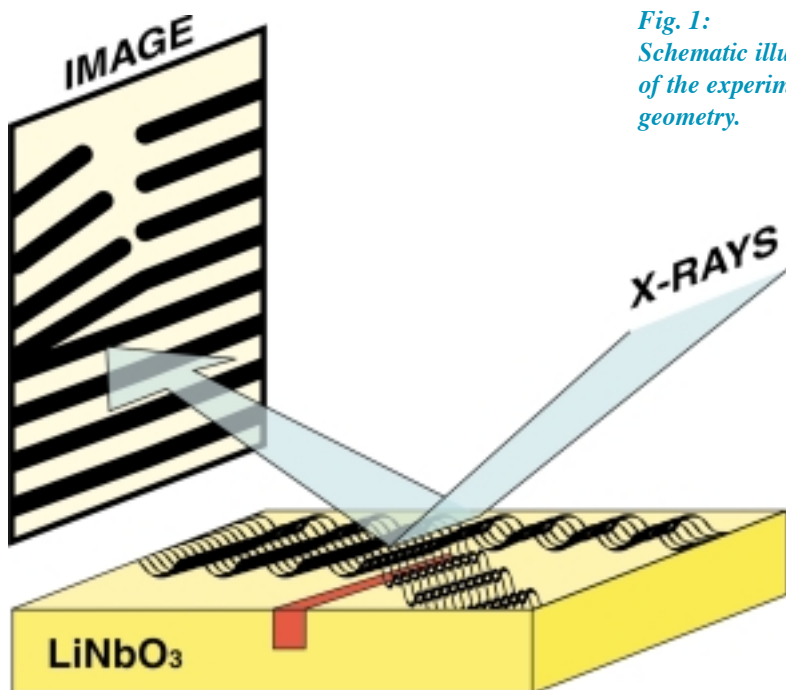


Fig. 1:
Schematic illustration of the experimental geometry.

X-ray diffraction imaging (x-ray topography) of the wavefronts has, in the past, been achieved for 30 MHz (wavelength $\sim 100 \mu\text{m}$) SAWs [1, 2]. The new possibilities provided by the ESRF allow to overcome the spatial resolution limitations encountered by the previous authors, and extend the visualization of SAW wavefronts to the frequency range presently used for the applications. The sample is a high-frequency ($\nu = 290\text{-}350 \text{ MHz}$, wavelength $\sim 10 \mu\text{m}$) LiNbO_3 -based SAW device, featuring a thin near-surface waveguide layer produced by the He ion implantation (Figure 1).

Traveling SAWs cause a long-range variation of elastic strain, which at any instant exhibits spatial periodicity over the whole crystal area. The modification of the x-ray intensity under SAW excitation is due to the corrugation of initially flat atomic planes. Stroboscopic diffraction imaging provides a "snapshot" of the SAW propagation, by accumulating images recorded at a given phase of the period. This was carried out by using an electrical signal associated with the pulsed x-ray beam from the storage ring

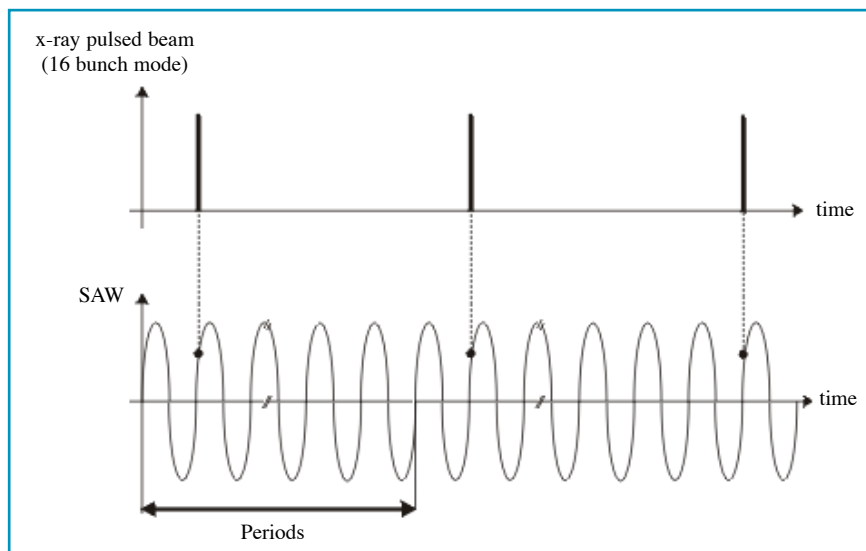
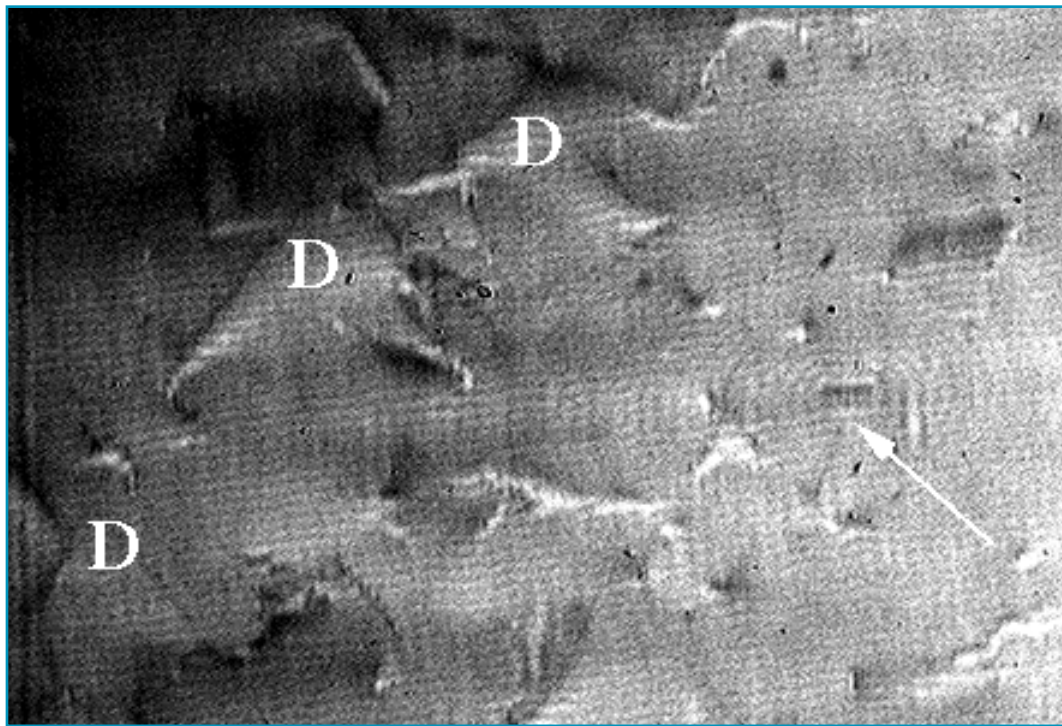


Fig. 2: Principle of stroboscopic diffraction imaging: the x-ray pulses always correspond to the same phase of the SAW at a given point of the crystal surface, allowing to sum up the diffracted beams up to required exposure time.



Fig. 3: Stroboscopic x-ray topograph of an as-implanted LiNbO₃ crystal (He ion energy - 320 keV, dose - $2 \cdot 10^{16} \text{ cm}^{-2}$) under SAW excitation. Crystal-film distance 23 cm. The acoustic ruler, introducing a 10- μm scale into the image, corresponds to the SAW wavefronts. Dislocations are indicated by the letters D. The location of the scattering center giving rise to secondary circular waves is indicated by an arrow.



operated in the 16-bunch mode, multiplied in frequency by an integer to drive the SAW device in a phase-locked mode, as schematically indicated on Figure 2.

X-ray topography was performed at the ID19 beamline, in the 16-bunch mode ($\nu_r = 5.68 \text{ MHz}$), *in situ*, under SAW excitation ($n = 51 \times \nu_r = 289.68 \text{ MHz}$ or $\nu = 62 \times \nu_r = 352.16 \text{ MHz}$). The images taken from such a modulated structure showed individual SAW wavefronts (alternating bright and dark lines, passing like a ruler through the image), as well as wavefront distortions, caused by basal screw dislocations D, as can be seen in Figure 3.

In addition, another scattering object, which we believe to be a He bubble, is visible in Figure 3 due to the secondary circular waves it produces. Secondary waves propagate away (at a distance of hundreds of micron) from the scattering center, like the waves that radiate from a stone plunged into water. A magnified picture of the circular elastic waves emanating from one of the bubbles is shown in Figure 4.

In fact ion implantation into single crystals is an important process in microelectronic and optoelectronic device technologies. It produces strain and defects within a thin layer buried at the ion stopping depth. Very small

defects, such as submicron bubbles, may affect the device characteristics even though they are invisible on standard x-ray topographs. It was found that a combination with short-wavelength SAWs results in an enhancement of the x-ray topographic contrast. When SAWs cross crystal regions containing extended defects, the individual wavefronts are distorted due to the scattering of acoustic power. Correspondingly, the acoustic ruler in the x-ray image becomes bent (see Figure 1), revealing defects which are not visible without the SAW. In the case of bubbles or cavities, which affect SAWs as strong density perturbations, secondary elastic waves arise, facilitating defect visualization.

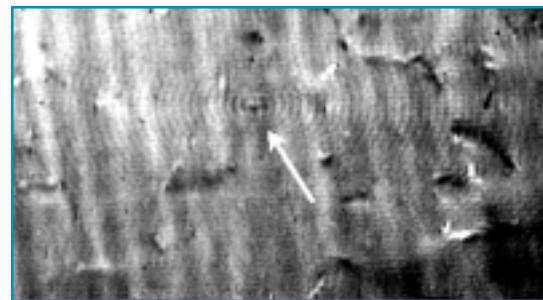


Fig. 4: X-ray topograph showing a picture of the secondary circular waves diverging from a He bubble (indicated by an arrow).

Analysis of all the collected images showed that the bubbles in our samples are 300-400 μm away from each other. The formation of a bubble thus appears to be a rare event, difficult to visualize except when benefiting from this "see-SAW" stroboscopic x-ray diffraction imaging technique [3]. ■

REFERENCES

- [1] R.W. Whatmore, P.A. Goddard, B.K. Tanner, G.F. Clark, *Nature* **299**, 44 (1982)
- [2] H. Cerva, W. Graeff, *Phys. Status Solidi A* **82**, 35 (1984)
- [3] E. Zolotoyabko, D. Shilo, W. Sauer, E. Pernot, J. Baruchel, *Appl. Phys. Lett.* **73**, 2278 (1998)